BJES Basrah Journal for Engineering Sciences

Basrah Journal for Engineering Sciences, Vol. 26, No. 1, (2026), 44-51

Original Article

Journal homepage: https://bjes.edu.iq/bjes
ISSN (Online): 23118385, ISSN (Print): 18146120

IRAQI Academic Scientific Journals

Experimental Study of Thermal Conductivity and Glass Transition Temperature of Epoxy/AI_2O_3 Composites

Shams J. Mohammed [1]*, Abdul Kareem F. Hassan [2]

[1]*Mechanical Engineering Department, College of Engineering, University of Basrah, Basrah, Iraq*
[2] *College of Engineering, Almaaqal University, Basrah, Iraq*
E-mail addresses: pgs.shams.aleidani@uobasrah.edu.iq , abdulkareem.flaih@almaaqal.edu.iq

Article Info

Article history:
Received: 14 February 2026
Revised: 11 May 2026
Accepted: 20 May 2026
Published: 28 July 2026

Keywords:
Epoxy composites, Alumina filler, Thermal conductivity, DSC, Glass transition temperature.

https://doi.org/10.33971/bjes.26.1.6

Abstract

This study aims to evaluate the effect of adding alumina particles at specific ratios on the thermal properties of the epoxy-alumina composite. The hand lay-up technique was employed using a gravity molding process. Six samples' specimens with dimensions specified by the International Standard (ASTM) were prepared with the specified volume ratios of alumina (0%, 10%, 20%, 40%, 50%, and 60%). X-Ray Diffraction (XRD) was conducted, and according to the Lee's principle the thermal conductivity was measured. The results showed that increasing the concentration of the alumina filler significantly enhances the thermal conductivity of the composite, reaching approximately 1.25 W/m.K at a loading of 60%. Moreover, the differential scanning calorimetry (DSC) analysis of the DSC conducted on samples containing (0%, 40%, and 60% AI_2O_3) only shows that the glass transition temperature (T_g) gradually increases with the increase in alumina content, reaching 138.92°C at 60% AI_2O_3. These results confirm the suitability of the developed composite for efficient thermal management in advanced engineering applications.

1. Introduction

The rapid advancement of electronic devices, electrical insulation systems, and power-intensive technologies has imposed increasingly stringent requirements on materials capable of efficient thermal management while maintaining mechanical integrity and electrical reliability. In many modern applications, including power electronics, high-voltage insulation, and electronic packaging, inadequate heat dissipation remains a primary factor limiting performance, reliability, and service lifetime. Consequently, the development of polymer-based materials with enhanced thermal conductivity, thermal stability, and processability has become a critical research priority.

Among polymer matrices, epoxy resins are widely employed due to their excellent adhesion, chemical resistance, dimensional stability, and favorable electrical insulation properties [1]. However, pristine epoxy exhibits inherently low thermal conductivity, which restricts its applicability in thermally demanding environments. To overcome this limitation, the incorporation of thermally conductive ceramic fillers has emerged as an effective and scalable strategy. In particular, aluminum oxide (AI_2O_3) has attracted considerable attention owing to its high intrinsic thermal conductivity, electrical insulation capability, chemical inertness, and cost-effectiveness. By tailoring filler loading, morphology, and interfacial characteristics, epoxy–AI_2O_3 composites offer a promising pathway toward multifunctional materials that simultaneously address thermal transport and thermal stability requirements, thereby motivating the extensive research efforts reviewed in the following section.

Ding et al. [2] offered an extensive design to epoxy-based thermal interface materials (TIMs), including alumina fillers, where a systematic review was applied to compare the impact of filler morphology, loading fraction, and enhancement strategies, including thermal network construction and minimization of interfacial thermal resistance, on thermal conductivity. The main results prove the fact that epoxy-AI_2O_3 systems have a good balance between being cost-effective and stable in the chemical properties, though the enhancement of thermal conductivity is rather limited by interfacial thermal resistance and filler agglomeration with high concentrations. The biggest drawback of the study is that it uses aggregated literature data with no strict standardization of the measurement techniques or conditions of processing, and thus, it does not provide direct quantitative comparisons between various studies.

Huang et al. [3] investigated the impact of filler morphology, especially the alumina nanowires, on the physicochemical characteristics of epoxy composites experimentally. The alumina nanowires were prepared and added to the epoxy matrix at various mass concentrations. The characterizations carried out later included thermal conductivity, dielectric properties and electrical breakdown strength. The major results were a significant increase in thermal conductivity with a corresponding increase in filler loading, reaching approximately 134 per cent at 10 wt. There were non-monotonic changes in the measured electrical parameters; volume resistivity was first increasing and then

decreasing whereas breakdown strength was initially increasing and then decreasing at higher concentrations of the filler. These findings highlight the sensitivity of the material performance to the complex interaction between the evolution of thermal transport networks and localization of electric fields or heat. Limitations of the study include the small set of filler loadings studied, which might not extend to the higher concentrations typically used in thermal interface material applications, and the largely qualitative study of the dispersion and agglomeration without a quantitative correlation to the underlying thermal network structure. Lee Sánchez et al. [4] adopted a clear experimental approach to enhance thermal conductivity using a hybrid filler system consisting of two-dimensional Boron Nitride (BN) flakes and zero-dimensional spherical AI_2O_3 particles, supported by extensive characterization including FTIR, viscosity, morphology, Coefficient of Thermal Expansion (CTE), glass transition temperature (T_g), decomposition temperature (T_d), dielectric properties, and thermal imaging. The most significant outcome was a substantial increase in thermal conductivity, reaching approximately 1.72 W/m.K at 80 wt.% filler content, corresponding to about a 7.8-fold enhancement compared to pristine epoxy. The study also tracked the influence of hybrid fillers on thermomechanical properties relevant to electronic encapsulation. However, the extremely high filler loading markedly increases viscosity and complicates industrial processability, and the presence of BN makes it difficult to isolate the specific contribution of AI_2O_3 if the research focus is solely on epoxy–alumina systems.

Long et al. [5] used branched alumina (b-AI_2O_3) fillers to create more bridging thermal conduction pathways in an epoxy material. The experimental process involved the preparation of branched alumina by the sintering method, the further preparation of composites with high filler content and the total measurement of thermal conductivity, electrical and dielectric characteristics. The findings showed that the branched architecture enables the formation of quasi-continuous thermal networks, which decreases interfacial resistance and significantly increases thermal conductivity, about ~1.13 W/m.K at 70 wt.%, which is almost seven times higher than unfilled epoxy, and also maintains desirable electrical insulation properties. The paper is aware of some of the limitations such as reliance on special filler preparation methods and the requirement of very high loading fractions, which can present limitations in terms of material density, process viability, and reproducibility. In addition, the composites are highly sensitive to the filler distribution and network integrity. Singh and Pandey [6] A key strength of this study is that it goes beyond measuring the composite's effective thermal conductivity and attempts to extract the thermal conductivity of the interphase itself. A hybrid methodology was employed, combining TPS 500 thermal conductivity measurements with a finite element model of a virtual composite over a range of assumed interphase conductivities, followed by an optimization algorithm to identify the interphase value. The principal finding revealed that the interphase may exhibit significantly higher thermal conductivity than the base polymer, indicating that interfacial engineering is a governing factor in heat transport rather than a secondary effect. The main limitation is that the interphase is often modeled using simplified assumptions of uniformity and effective thickness. In contrast, real systems may exhibit gradients and local heterogeneities that depend on processing and surface chemistry. Pan et al. [7] investigated the dispersion of AI_2O_3 particles of different sizes in an epoxy matrix and its effect on thermal conductivity. Epoxy composites filled with AI_2O_3 particles of varying sizes and contents were prepared to evaluate their thermal performance. The results showed that nanoparticles of approximately 30 nm were uniformly dispersed within the epoxy matrix, leading to the formation of effective conductive pathways and achieving a maximum thermal conductivity of 2.52 W/m.K. However, larger particle sizes (greater than 17 μm) resulted in particle agglomeration and increased surface roughness, which negatively affected heat transfer by disrupting the formation of continuous conduction pathways. Xu et al. [8] examined how epoxy/AI_2O_3 composites are influenced by varying alumina particle sizes when micro-AI_2O_3 with various particle sizes (5, 10, 40, 60, and 120 μm) has been utilized as a thermally conductive filler for the epoxy resin composite. Stress and strain tests have been done simultaneously to determine the mechanical properties. It found that from the results, as the size of the alumina particles increased, the thermal conductivity reduced with the same quantity of alumina filling. This suggests that smaller particles increase heat conductivity. The thermal conductivity and T_g (glass transition temperature) of epoxy/AI_2O_3 composite material decrease with the increase of alumina particle size. Also, when the size of the alumina particles increased, the epoxy/AI_2O_3 composite's energy storage modulus increased as well, reaching the peak at 160 MPa. This implies that the mechanical strength of the composite is positively impacted by bigger particles.

Xie and Yang [9] explained an atomistic perspective with respect to the effect of dimensions of Al_2O_3 nanoparticle (between 1 to 1.5 nm) on the characteristics of an epoxy system, using molecular dynamics simulations of a DGEBF matrix which was further cross-linked with DETDA at a constant volume fraction. The results showed that when small nanoparticles are added, the values of the glass transition temperature and the elastic modulus are increased, accompanied by a decrease in the coefficient of thermal expansion. It was these improvements that were credited with an increase in cohesive energy density and a resulting limitation of polymer chain mobility that was shown by a lower mean square displacement. The results therefore support the assumption that nanoscale interfacial processes can strengthen thermomechanical stability. Nevertheless, one of the main weaknesses lies in the fact that the model of molecular dynamics simulations is an idealized system with perfect dispersion and limited time and space scales; therefore, it does not directly provide experimental measurements of thermal conductivity or entirely realistic agglomeration effects.

Farhan and Hussein [10] studied the effect of alumina particle loading on the mechanical properties of polymer composites. Polyester-based composites containing 0–5 wt.% alumina particles (50 μm) were prepared and evaluated through impact, compression, tensile, hardness, and flexural tests. The results showed that the mechanical performance improved with uniform particle distribution within the matrix. The composite containing 5 wt.% alumina exhibited a significant increase in impact strength (about 82.74%) and hardness compared to the unfilled matrix. In addition, moderate improvements in tensile strength were observed at lower filler contents (1–3 wt.%), indicating a strong relationship between alumina content and impact resistance.

Paul et al. [11] this review gave an applied and diagnostic outlook on epoxy nanocomposites in electrical insulation using a systematic approach that correlates the improvement of thermal and dielectric characteristics with the quality of dispersion and with the best filler loading before the agglomeration effect and the resulting dielectric losses occur. The major conclusion was that the optimal filler ratio and quality of the interfaces between the fillers and the matrix are the determinants of high performance without an upsurge in the dielectric loss. This is the limitation because the review is not limited to any one type of filler, as it is more focused on epoxy and AI_2O_3 fillers.

Despite the extensive efforts reported in the literature to enhance the thermal conductivity of epoxy–AI_2O_3 systems, most studies either rely on hybrid fillers, focus on micro/nanoscale modeling, or emphasize functional insulation performance rather than providing a systematic experimental correlation between filler loading, thermal conductivity enhancement, and thermal stability. In this context, the present study aims to experimentally investigate the thermal conductivity and glass transition behavior of epoxy–Al_2O_3 composites over a wide filler loading range, offering direct insight into the coupled evolution of heat transport and thermal stability.

2. Materials and methods

2.1. Composite materials

Sikadur® 52 LP low-viscosity injection resin Appendix-A, has been used as the matrix material, it is a high-strength with two component A and B, with a convenient, easy mixing ratio A:B = 2:1 by volume, moisture-tolerant. Formulated specifically for grouting both dry and damp cracks. It conforms to the current ASTM C-881, types I and II, grade-1, class C, and AASHTO M-235 specifications.

White fused alumina with an average grain size of 50 µm was used as the reinforcement material.

Table 1 presents the most important characteristics [12],[13].

Table 1. Most important mechanical and thermal properties of epoxy and alumina.

Property	Epoxy	Alumina
Color	Clear, Pale yellow	White
Ultimate tensile strength	54 MPa	220 MPa
Poisson's coefficient (ν)	0.389	-
Density (A + B)	1.06 kg/L	-
Thermal conductivity	-	35 W/m.K
Heat deflection temperature (ASTM D-648)	122°F (50°C)	-

2.2. Composite fabrication method

Epoxy/alumina composites were fabricated using the hand lay-up technique [14]. Initially, the required volume of epoxy resin was measured and mixed with the hardener in a predetermined ratio 2:1 and stirred thoroughly to ensure uniform mixing. Alumina particles were added to the epoxy-hardener mixture at predetermined volume fractions (0%, 10%, 20%, 40%, 50%, and 60 wt.%). The mixture was then stirred by hand using a glass stirring rod for a period of 5 to 15 minutes to promote uniform dispersion of alumina particles within the epoxy matrix. To minimize air entrapment and improve wetting of the filler, the mixture was gently stirred at low speed, with using the hot water immersion method. After achieving a homogeneous mixture, the composite mixtures were poured into a disk-shaped Teflon mold Fig. 1.

The design and fabrication of the Teflon mold were performed in the Science Camp Fab Lab.

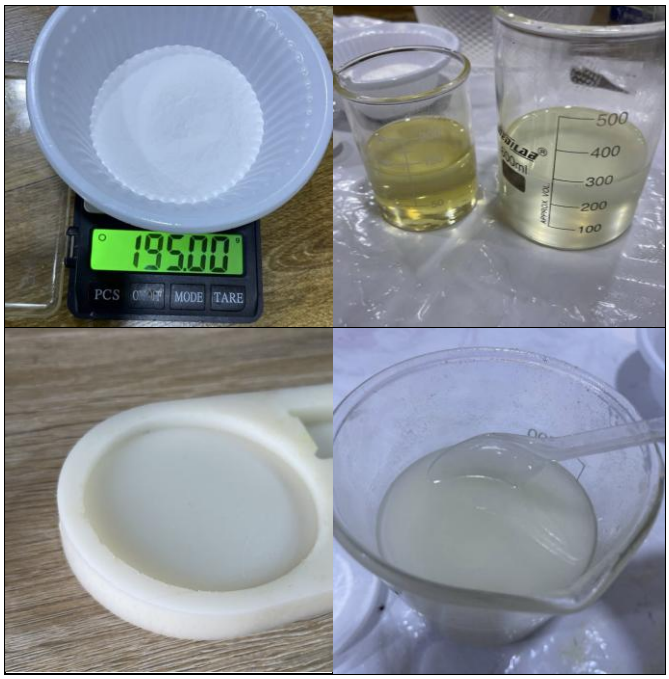

Fig. 1 epoxy/Al_2O_3 composite preparation.

2.3. Specimen preparation

The poured mixtures were cured at room temperature for the specified curing period, approximately 24 hours to ensure complete cross-linking of the epoxy matrix. The obtained specimens were disk-shaped (76.2 mm diameter and 6 mm thickness) in accordance with the requirements of the testing device that operates according to the general guidelines of ASTM D7340 [15], as shown in Fig. 2.

Fig. 2 composite disk specimens.

The experimental procedure was repeated with the six different mixing ratios of epoxy and alumina. As shown in Table 2.

Table 2. volume calculation for all epoxy and AI_2O_3 ratios.

Fraction volume %		Volume (cm^3)		
Al_2O_3	Epoxy	A	B	Al_2O_3
0	100	18.233	9.117	0.000
10	90	16.410	8.205	2.735
20	80	14.587	7.293	5.47
40	60	10.940	5.470	10.94
50	50	9.117	4.558	13.675
60	40	7.293	3.647	16.410

3. Experimental tests

3.1. X-Ray diffraction (XRD)

The methods of phase analysis [16], the structural properties of the epoxy-alumina composites have been investigated using an X-Ray Diffraction (XRD) diffractometer using Cu-K alpha radiation. Two samples, pure epoxy and epoxy reinforced with 60% alumina, were measured. At a measurement temperature of 25 °C, the diffraction patterns were captured throughout a 2θ range of 10°–80° with a step size of 0.1° and a scanning time of 2 s per step.

3.2. Thermal properties

3.2.1. Thermal conductivity

Lee's disc technique, which was carried out in accordance with the ASTM C518-02 standard [17], is used to determine the thermal conductivity of the samples examined in this study, which is based on Fourier's theory of heat conduction, Eq. (1) [18].

$$\frac{dT}{dx}k = -\frac{q}{A} \tag{1}$$

The equation represents the case of one-dimensional heat transfer along the *x*-direction, the conductive heat flux per unit area *q*/*A*, *A*: can be expressed in terms of an elemental thickness *dx* across which a temperature difference *dT* exists. *k* is the thermal conductivity, W/m.K, *dT/dx* is heat transfer along the *x*-direction at a steady-state temperature, K/m. *A* is the cross-sectional area in m^2. The equation's negative sign indicates that heat is flowing in the direction of a falling temperature.

The specimens of the material are to be tested in the form of a disc placed between two brass discs, as shown in Fig. 3. The thermal conductivity of the composite samples was determined, expressed by Eq. (2).

$$k = \frac{m_{C_p}\dfrac{dT}{dt}}{(T_1 - T_2)A} \tag{2}$$

Where m is the mass of the brass disk in kg, C_p is the brass disk specific heat capacity J/kg.K, *dT/dt* rate of temperature change over time K/s. T_1 and T_2 are the temperature differences between the two discs.

Fig. 3 The laboratory setup of Lee's apparatus.

3.2.2. Differential scanning calorimetry (DSC)

Differential Scanning Calorimetry (DSC) is a thermal analysis technique in which the difference in heat flow between a sample and a reference is measured as a function of temperature [19]. In this study, DSC was used to evaluate the thermal behavior of epoxy–Al_2O_3 composites with varying amounts of filler, and determine the glass transition temperature (T_g) of the composite samples (T_g). The analysis was conducted on three samples (0%, 40%, and 60 wt.% Al_2O_3) using a Shimadzu DSC-60 instrument, as shown in Fig. 4, in accordance with ASTM D3418 [20] and ISO 11357 standards. About 5–10 mg of the composite powder was sealed in high-purity metal DSC pans. Measurements were performed under a nitrogen atmosphere at a heating rate of 10 °C/min over a temperature range of 25–350 °C.

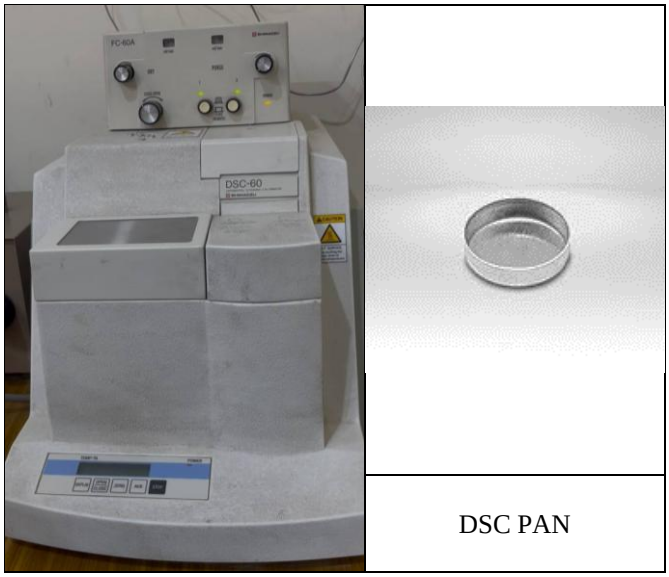

Fig. 4 DSC testing device.

4. Results and discussion

4.1. XRD result

The obtained XRD patterns are shown in Figs. 5, and 6.

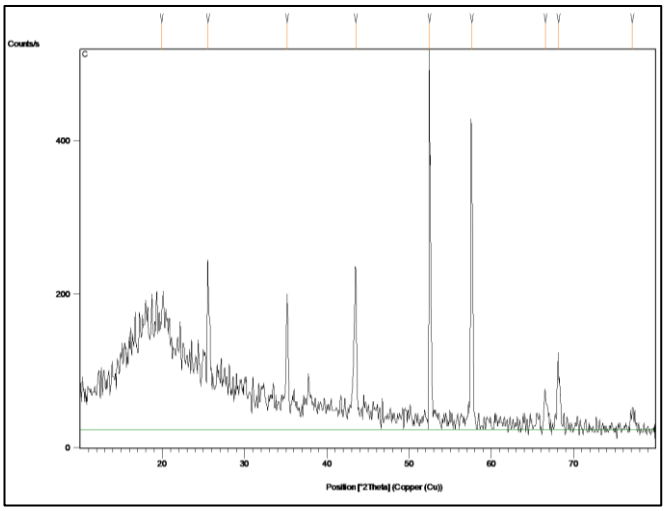

Fig. 5 XRD pattern of pure epoxy specimen.

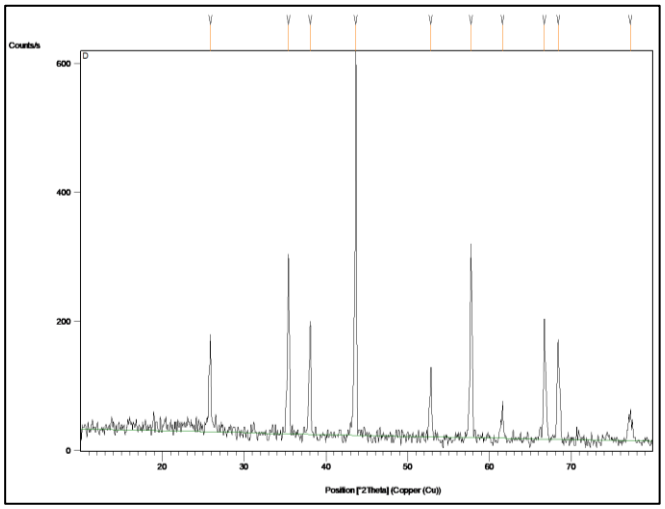

Fig. 6 XRD pattern of 60 wt.% Al_2O_3 specimens.

As reported by Khan et al. [21], the XRD pattern of the pure epoxy specimen was explained by a broad diffuse halo with no distinct diffraction peaks, refer to the amorphous nature of the epoxy resin due to the absence of long-range crystalline order and the random arrangement of polymer chains. In contrast, the epoxy–alumina composite exhibits several sharp and well-defined diffraction peaks across the scanned 2θ range. These peaks are attributed to the crystalline structure of alumina AI_2O_3, confirming the successful incorporation of alumina particles into the epoxy matrix. The high alumina content 60 wt.% dominates the diffraction response of the composite, as reflected by the high intensity and sharpness of the observed peaks. Furthermore, the XRD results confirm the phase purity of the AI_2O_3 filler, as no additional or unexpected peaks were detected. The absence of peak shifting or the phases indicates that no chemical reaction occurred between the epoxy matrix and the alumina particles during processing. This suggests that the composite system is primarily a physical mixture, with alumina particles well-dispersed within the polymer matrix.

4.2. Thermal test results

4.2.1. Thermal conductivity

The thermal conductivity values of Epoxy-Alumina composites are presented in Table 3 and Fig. 7.

Table 3. Epoxy-Alumina composites thermal conductivity results.

Sample no.	Composite composition	Thermal conductivity (K) W/m.K
1	100% epoxy	0.154
2	90% Epoxy, 10% Alumina	0.293
3	80% Epoxy, 20% Alumina	0.402
4	60% Epoxy, 40% Alumina	0.731
5	50% Epoxy, 50% Alumina	1.043
6	40% Epoxy, 60% Alumina	1.274

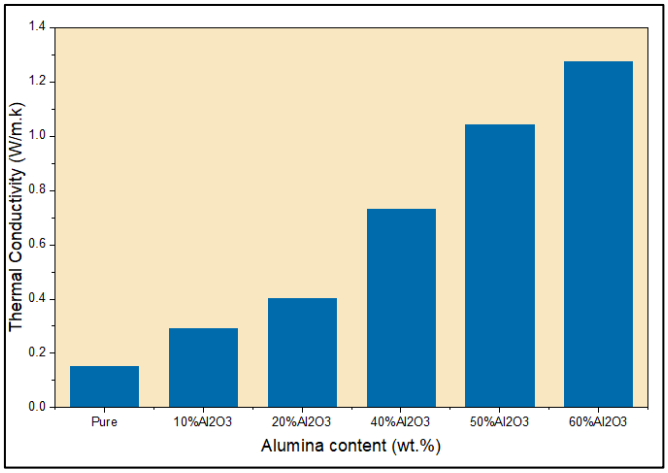

Fig. 7 The thermal conductivity of the six specimens of epoxy–Al_2O_3 composites.

The results show a pronounced increase in thermal conductivity with increasing alumina loading. The thermal conductivity of the pure epoxy is relatively low (≈ 0.15 W/m.K), which is attributed to the complex morphology of polymer chains and the limited phonon transport within the amorphous matrix. In general, the thermal conductivity of particulate-filled composites is governed by the filler–matrix coupling, interfacial thermal resistance, as well as the concentration and geometric characteristics of the fillers [22]. At low filler concentrations, no continuous inter-filler networks are formed; therefore, the enhancement in thermal conductivity is limited. With the incorporation of alumina particles, the thermal conductivity increases progressively, reaching approximately 1.25 W/m.K at 60 wt.% AI_2O_3. This significant improvement can be attributed to the intrinsically high thermal conductivity of alumina and the formation of continuous heat-conduction pathways within the composite at higher filler loadings. Where, in greater filler loadings, the interparticle distance reduces, increasing particle interaction and lowering thermal resistance across the epoxy-alumina interface [23].

The observed trend is consistent with previous studies reported in the literature, as it was reported in the work of Zhou et al. [24], confirming the effectiveness of ceramic fillers in enhancing the thermal transport properties of polymer-based composites.

4.2.2. Differential scanning calorimetry result

The results appear an increase in the glass transition temperature (T_g) with increasing alumina content, as summarized in Table 4 and Fig. 8.

Table 4. Epoxy-Alumina composites DSC results.

Sample no.	Composite composition	Tg (°C)
1	100% Epoxy	80.76
2	60% Epoxy, 40% Alumina	95.07
3	40% Epoxy, 60% Alumina	120.82

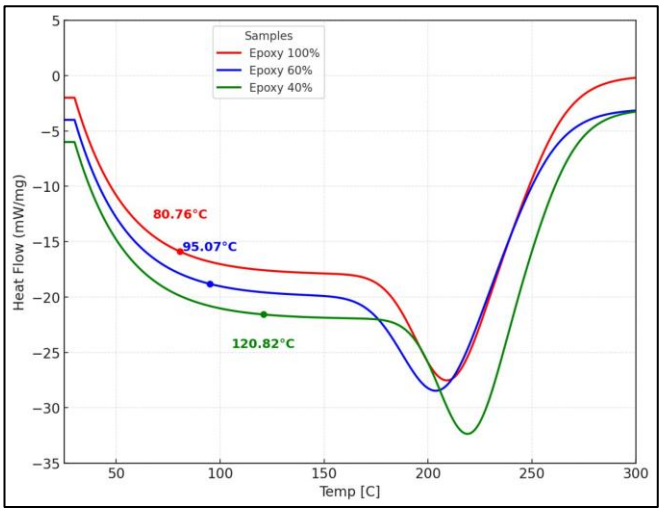

Fig. 8 DSC thermograms for glass transition temperature (T_g).

Three characteristic temperatures can be identified from the DSC curves: the onset, midpoint, and end temperatures. In this study, the midpoint temperature is taken as the glass transition temperature (T_g).

The curve we obtained shows that the pure epoxy exhibits the lowest (T_g) value, and this is because the glass transition temperature (T_g) is closely related to the cross-linking density of the polymer network due to the non-uniform cross-linking within the epoxy matrix [25]. While there was a systematic increase in (T_g) with increasing alumina content exhibit its highest values for 40 wt.% and 60 wt.% AI_2O_3, This behavior can be attributed to the restriction of polymer chain mobility caused by the rigid alumina particles and the enhanced interfacial interactions between the filler and epoxy matrix [26], since the stiff alumina particles limit the movement of epoxy molecular chains and decrease the free volume [8], which makes the glass transition require more energy to occur. The limited mobility of matrix chain segments, the development of a rigid interphase at the filler–matrix interface, and changes in the local crosslink density close to the dispersed particles represent a few of the mechanisms that explain the beneficial effect of alumina on the T_g of epoxy composites [26]. Strong connections between the AI_2O_3 particles and the epoxy network have been linked to the increase in T_g seen at larger alumina loadings [25]. These contacts reduce the segmental mobility of the chains, raising the glass transition temperature [8]. The addition of alumina enhances the epoxy matrix's heat stability and fortifies the polymer network.

5. Conclusions

This study examined the effect of Alumina particles on epoxy composites subjected to tests of thermal conductivity and DSC, the following conclusions were drawn:

The present study successfully fabricated epoxy/AI_2O_3 composites with filler contents ranging from 10 to 60 % by volume, demonstrating that alumina particles were physically bonded within the epoxy matrix without strong interfacial interaction. A relatively homogeneous microstructure was achieved at low to moderate filler loadings, whereas higher alumina contents led to noticeable particle agglomeration. Structural analysis using XRD confirmed the amorphous nature of pure epoxy, while the composites exhibited distinct crystalline peaks corresponding to alumina, with the 60 vol.% sample showing dominant and sharp peaks that indicate the effective incorporation and prevalence of the ceramic phase. Thermally, the addition of alumina significantly enhanced the thermal conductivity, reaching a maximum value of 1.274 W⁄m.K at 60 vol.% due to the formation of continuous heat conduction pathways facilitated by the high intrinsic conductivity of alumina. Furthermore, DSC analysis revealed a progressive increase in the glass transition temperature (T_g) with increasing filler content, achieving a maximum improvement of 49.6% at 60 vol.% alumina, which reflects restricted polymer chain mobility. Overall, the results highlight that alumina loading plays a critical role in tailoring the thermal performance of epoxy composites; however, an optimal filler content must be carefully selected to balance improved stiffness and thermal conductivity against potential drawbacks such as particle agglomeration and reduced toughness.

References

[1] J. A. Gannon, “History and Development of Epoxy Resins,” In: Seymour, R.B., Kirshenbaum, G.S. (eds) High Performance Polymers: Their Origin and Development. Springer, Dordrecht, 1986. https://doi.org/10.1007/978-94-011-7073-4_29

[2] T. Ding, W.-X. Ma, and Z.-B. Zhao, “Review of Alumina-Based Filler/Epoxy Resin Composites for Thermally Conductive Materials,” Polymer Engineering & Science, vol. 66, no. 2, pp. 648-661, 2026. https://doi.org/10.1002/pen.70251

[3] L. Huang, X. Lv, Y. Tang, G. Ge, P. Zhang, and Y. Li, “Effect of Alumina Nanowires on the Thermal Conductivity and Electrical Performance of Epoxy Composites,” Polymers, vol. 12, Issue 9, 2020. https://doi.org/10.3390/polym12092126

[4] W. A. Lee Sanchez, C.-Y. Huang, J.-X. Chen, Y.-C. Soong, Y.-N. Chan, K.-C. Chiou, T.-M. Lee, C.-C. Cheng, and C.-W. Chiu, “Enhanced Thermal Conductivity of Epoxy Composites Filled with Al_2O_3/Boron Nitride Hybrids for Underfill Encapsulation Materials,” Polymers, vol. 13, Issue 1, 2021. https://doi.org/10.3390/polym13010147

[5] Y. Long, L. Shi, Q. Wang, H. Qu, C. Hao, and Q. Lei, “Effect of branched alumina on thermal conductivity of epoxy resin,” Journal of Industrial and Engineering Chemistry, vol. 120, pp. 209-215, 2023. https://doi.org/10.1016/j.jiec.2022.12.027

[6] M. Singh, and J. C. Pandey, “Probing thermal conductivity of interphase in epoxy alumina nanocomposites,” Polymers and Polymer Composites, vol. 30, 2022. https://doi.org/10.1177/09673911221077489

[7] Z. Pan, Y. Liu, F. Wang, G. Lu, F. Yang, and F. Cheng, "Al_2O_3 dispersion-induced micropapillae in an epoxy composite coating and implications in thermal conductivity," ACS Omega, vol. 6, Issue 28, pp. 17870-17879, 2021. https://doi.org/10.1021/acsomega.1c01282

[8] Z. Xu, C. Zhang, Y. Li, J. Zou, Y. Li, B. Yang, R. Hu, and Q. Qian, "Effect of the alumina micro-particle sizes on the thermal conductivity and dynamic mechanical property of epoxy resin," PLOS ONE, vol. 18, Issue 10, e0292878, 2023. https://doi.org/10.1371/journal.pone.0292878

[9] X. Xie and D. Yang, "Multi-functionalization of Al_2O_3 nanoparticles for enhancing thermal conductivity of epoxy natural rubber composites," Applied Surface Science, vol. 602, no. 154335, 2022. https://doi.org/10.1016/j.apsusc.2022.154335

[10] A. J. Farhan and W. A. Hussein, "Effect of alumina contents on some mechanical properties of alumina (Al_2O_3) reinforced polymer composites," NeuroQuantology, vol. 18, no. 5, pp. 35–42, 2020. https://doi.org/10.14704/nq.2020.18.5.NQ20165

[11] S. K. Paul, S. Maur, S. Biswas, and A. K. Pradhan, "Review on Thermal and Electrical Properties for Condition Assessment of Epoxy Nano- Composites by Advanced Techniques," IEEE Transactions on Dielectrics and Electrical Insulation, vol. 31, Issue 1, pp. 230-245, 2024. https://doi.org/10.1109/TDEI.2023.3313995

[12] Y. Xing, J. Zheng, and Y. Feng, "Molecular Dynamics Simulation of Epoxy/Al_2O_3 Nanocomposites as Insulation Material for High Temperature Superconducting Insulation," International Journal of Electrochemical Science, vol. 17, Issue 9, p. 220933, 2022. https://doi.org/10.20964/2022.09.12

[13] M. Mohamed, S. Brahma, H. Ning and S. Pillay, "Development of beneficial residual stresses in glass fiber epoxy composites through fiber prestressing," Journal of Reinforced Plastics and Composites, vol. 39, Issue 13-14, pp. 487-498, 2020. https://doi.org/10.1177/0731684420916534

[14] R. R. Nagavally, "Composite Materials - History, Types, Fabrication Techniques, Advantages, and Applications," International Journal of Current Research, vol. 8, Issue 9, pp. 37763-37768, 2016.

[15] ASTM D7340-07 Standard Practice for Thermal Conductivity of Leather, 2023.

[16] J. Epp, "X-Ray Diffraction (XRD) Techniques for Materials Characterization," Materials Characterization Using Nondestructive Evaluation (NDE) Methods, pp. 81-124, 2016. https://doi.org/10.1016/B978-0-08-100040-3.00004-3

[17] ASTM C518-21 Standard Test Method for Steady-State Thermal Transmission Properties by Means of the Heat Flow Meter Apparatus, Sep 28, 2021.

[18] R. Karwa, Heat and Mass Transfer, Second Edition, Springer Nature Singapore Pte Ltd., 2020. ISBN 978-981-15-3987-9. https://doi.org/10.1007/978-981-15-3988-6

[19] J. D. Menczel and R. B. Prime, Thermal Analysis of Polymers: Fundamentals and Applications, April 2009. ISBN 978-0-471-76917-0.

[20] ASTM D3418-12e1 Standard Test Method for Transition Temperatures and Enthalpies of Fusion and Crystallization of Polymers by Differential Scanning Calorimetry.

[21] H. Khan, A. S. Yerramilli, A. D'Oliveira, T. L. Alford, D. C. Boffito, and G. S. Patience, "Experimental methods in chemical engineering: X-ray diffraction spectroscopy XRD," The Canadian Journal of Chemical Engineering, vol. 98, Issue 6, pp. 1255-1266, 2020. https://doi.org/10.1002/cjce.23747

[22] C. Huang, X. Qian, and R. Yang, "Thermal conductivity of polymers and polymer nanocomposites," Materials Science and Engineering: R: Reports, vol. 132, pp. 1-22, 2018. https://doi.org/10.1016/j.mser.2018.06.002

[23] W. Yu, and H. Xie, "A Review on Nanofluids: Preparation, Stability Mechanisms, and Applications," Journal of Nanomaterials, vol. 2012, Issue 1, 2011. https://doi.org/10.1155/2012/435873

[24] W. Zhou, S. Qi, C. Tu, H. Zhao, C. Wang and J. Kou, "Effect of the particle size of Al_2O_3 on the properties of filled heat-conductive silicone rubber," Journal of Applied Polymer Science, vol. 104, Issue 2, pp. 1312-1318, 2007. https://doi.org/10.1002/app.25789

[25] X. Wu, Y. Wang, L. Xie, J. Yu, F. Liu and P. Jiang, "Thermal and electrical properties of epoxy composites at high alumina loadings and various temperatures," Iranian Polymer Journal, vol. 22, pp. 61–73, 2013. https://doi.org/10.1007/s13726-012-0104-4

[26] J. P. B. Souza, J. M. L. Reis, L. A. Sphaier and D. C. Moreira, "A preliminary study of glass transition temperature on epoxy/alumina nanocomposites," Revista De Engenharia Térmica, vol. 13, no. 1, pp. 32-35, 2014. https://doi.org/10.5380/reterm.v13i1.62066

Appendix

Appendix-A Epoxy resin technical datasheet.

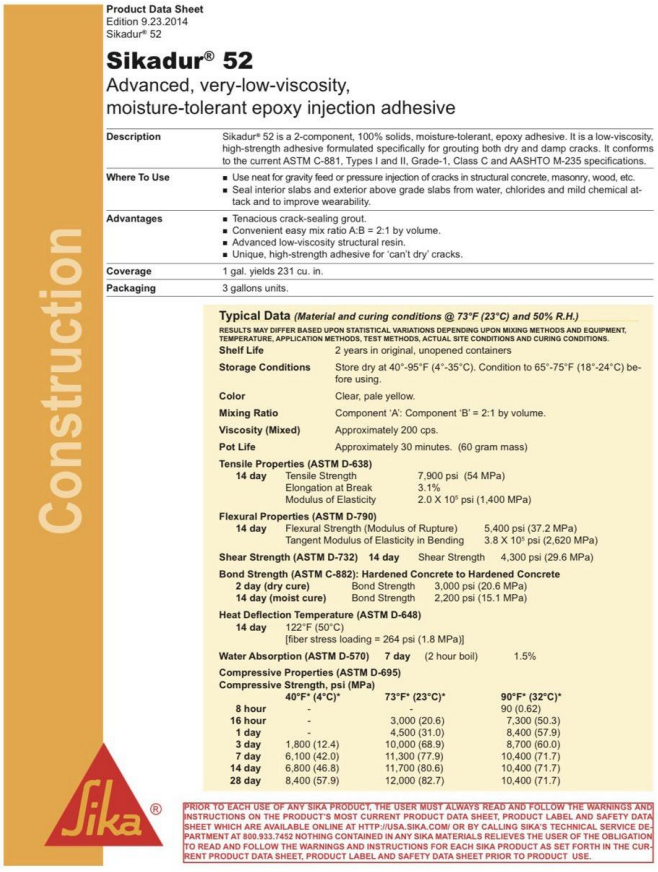

Product Data Sheet
Edition 9.23.2014
Sikadur® 52

Sikadur® 52

Advanced, very-low-viscosity, moisture-tolerant epoxy injection adhesive

Construction

Description	Sikadur® 52 is a 2-component, 100% solids, moisture-tolerant, epoxy adhesive. It is a low-viscosity, high-strength adhesive formulated specifically for grouting both dry and damp cracks. It conforms to the current ASTM C-881, Types I and II, Grade-1, Class C and AASHTO M-235 specifications.
Where To Use	▪ Use neat for gravity feed or pressure injection of cracks in structural concrete, masonry, wood, etc. ▪ Seal interior slabs and exterior above grade slabs from water, chlorides and mild chemical attack and to improve wearability.
Advantages	▪ Tenacious crack-sealing grout. ▪ Convenient easy mix ratio A:B = 2:1 by volume. ▪ Advanced low-viscosity structural resin. ▪ Unique, high-strength adhesive for 'can't dry' cracks.
Coverage	1 gal. yields 231 cu. in.
Packaging	3 gallons units.

Typical Data *(Material and curing conditions @ 73°F (23°C) and 50% R.H.)*

RESULTS MAY DIFFER BASED UPON STATISTICAL VARIATIONS DEPENDING UPON MIXING METHODS AND EQUIPMENT, TEMPERATURE, APPLICATION METHODS, TEST METHODS, ACTUAL SITE CONDITIONS AND CURING CONDITIONS.

Shelf Life 2 years in original, unopened containers

Storage Conditions Store dry at 40°-95°F (4°-35°C). Condition to 65°-75°F (18°-24°C) before using.

Color Clear, pale yellow.

Mixing Ratio Component 'A': Component 'B' = 2:1 by volume.

Viscosity (Mixed) Approximately 200 cps.

Pot Life Approximately 30 minutes. (60 gram mass)

Tensile Properties (ASTM D-638)

14 day	Tensile Strength	7,900 psi (54 MPa)
	Elongation at Break	3.1%
	Modulus of Elasticity	2.0 X 10^5 psi (1,400 MPa)

Flexural Properties (ASTM D-790)

14 day	Flexural Strength (Modulus of Rupture)	5,400 psi (37.2 MPa)
	Tangent Modulus of Elasticity in Bending	3.8 X 10^5 psi (2,620 MPa)

Shear Strength (ASTM D-732) 14 day Shear Strength 4,300 psi (29.6 MPa)

Bond Strength (ASTM C-882): Hardened Concrete to Hardened Concrete

2 day (dry cure)	Bond Strength	3,000 psi (20.6 MPa)
14 day (moist cure)	Bond Strength	2,200 psi (15.1 MPa)

Heat Deflection Temperature (ASTM D-648)
14 day 122°F (50°C)
[fiber stress loading = 264 psi (1.8 MPa)]

Water Absorption (ASTM D-570) 7 day (2 hour boil) 1.5%

Compressive Properties (ASTM D-695)

Compressive Strength, psi (MPa)

	40°F* (4°C)*	73°F* (23°C)*	90°F* (32°C)*
8 hour	-	-	90 (0.62)
16 hour	-	3,000 (20.6)	7,300 (50.3)
1 day	-	4,500 (31.0)	8,400 (57.9)
3 day	1,800 (12.4)	10,000 (68.9)	8,700 (60.0)
7 day	6,100 (42.0)	11,300 (77.9)	10,400 (71.7)
14 day	6,800 (46.8)	11,700 (80.6)	10,400 (71.7)
28 day	8,400 (57.9)	12,000 (82.7)	10,400 (71.7)

PRIOR TO EACH USE OF ANY SIKA PRODUCT, THE USER MUST ALWAYS READ AND FOLLOW THE WARNINGS AND INSTRUCTIONS ON THE PRODUCT'S MOST CURRENT PRODUCT DATA SHEET, PRODUCT LABEL AND SAFETY DATA SHEET WHICH ARE AVAILABLE ONLINE AT HTTP://USA.SIKA.COM/ OR BY CALLING SIKA'S TECHNICAL SERVICE DEPARTMENT AT 800.933.7452 NOTHING CONTAINED IN ANY SIKA MATERIALS RELIEVES THE USER OF THE OBLIGATION TO READ AND FOLLOW THE WARNINGS AND INSTRUCTIONS FOR EACH SIKA PRODUCT AS SET FORTH IN THE CURRENT PRODUCT DATA SHEET, PRODUCT LABEL AND SAFETY DATA SHEET PRIOR TO PRODUCT USE.

Construction

Compressive Modulus	**28 days**	3.5 x 10^6 psi (2,400 MPa)

* Material cured and tested at the temperatures indicated.

How to Use

Surface Preparation

Surface must be clean and sound. It may be dry or damp, but free of standing water. Remove dust, laitance, grease, curing compounds, impregnations, waxes and any other contaminants.

Preparation Work: Concrete - Should be cleaned and prepared to achieve a laitance and contaminant free, open textured surface by blast cleaning or equivalent mechanical means.

Steel - Should be cleaned and prepared thoroughly by blast cleaning or other equivalent mechanical means.

Mixing

Proportion 1 part Component 'B' to 2 parts Component 'A' by volume into a clean pail. Mix thoroughly for 3 minutes with Sika Paddle on low-speed (400-600 rpm) drill until uniformly blended. Mix only that quantity that can be used within its pot life.

Application

To gravity feed cracks - Blow vee-notched crack clean with oil-free compressed air. Pour neat Sikadur® 52 into vee-notched crack. Continue placement until cracks are completely filled. Prior to filling, seal underside of slab if cracks reflect through.

To pressure inject cracks - Use automated injection equipment or manual method. Set appropriate injection ports based on system used. Seal ports and cracks with Sikadur 31, Hi-Mod Gel, or Sikadur® 33.

When the epoxy adhesive seal has cured, inject Sikadur® 52 with steady pressure. Consult Technical Service for additional information.

To seal slabs - Spread neat mixture of Sikadur® 52 over slab using a roller or squeegee, working material thoroughly into the substrate to ensure penetration. Coverage should be uniform. Coat interior slabs and above-grade exterior slabs only.

Limitations

- Minimum substrate and ambient temperature 40°F (4°C).
- Do not thin. Addition of solvents will prevent proper cure.
- Material is a vapor barrier after cure.
- Not for injection of cracks under hydrostatic pressure at the time of application.
- Do not inject cracks greater than 1/4 in. (6 mm) without consulting Technical Service.
- Do not seal exterior slabs on grade.
- Not an aesthetic product. Color may alter due to variations in lighting and/or UV exposure.

Visit our website at usa.sika.com **1-800-933-SIKA NATIONWIDE**

Regional Information and Sales Centers. For the location of your nearest Sika sales office, contact your regional center.

Sika Corporation
201 Polito Avenue
Lyndhurst, NJ 07071
Phone: 800-933-7452
Fax: 201-933-6225

Sika Canada Inc.
601 Delmar Avenue
Pointe Claire
Quebec H9R 4A9
Phone: 514-697-2610
Fax: 514-694-2792

Sika Mexicana S.A. de C.V.
Carretera Libre Celaya Km. 8.5
Fracc. Industrial Balvanera
Corregidora, Queretaro
C.P. 76920
Phone: 52 442 2385800
Fax: 52 442 2250537